AFRL-VS-HA-TR-2005-1178

Mapping Near-Equatorial Particle Distributions to Higher Latitudes: Estimates of Accuracy and Sensitivity

Gregory P. Ginet

30 Nov 2005

AIR FORCE RESEARCH LABORATORY
Space Vehicles Directorate
29 Randolph Rd
AIR FORCE MATERIEL COMMAND
Hanscom AFB, MA 01731-3010

'AFRL-VS-HA-TR-2005-1178

This technical report has been reviewed and is approved for publication.

/ signed /
Gregory P. Ginet, DR-IV
Space Weather Center of Excellence

/ signed /
Joel B. Mozer, Chief
Space Weather Center of Excellence

/ signed /
Robert A. Morris, Chief
Battlespace Environment Division
Space Vehicles Directorate

REPORT DOCUMENTATION PAGE	*Form Approved* *OMB No. 0704-01-0188*

1. REPORT DATE *(DD-MM-YYYY)*	2. REPORT TYPE	3. DATES COVERED *(From - To)*
06-12-2005	Scientific, Interim	

4. TITLE AND SUBTITLE
Mapping Near-Equatorial Particle Distributions to Higher Latitudes: Estimates of Accuracy and Sensitivity

5a. CONTRACT NUMBER

5b. GRANT NUMBER

5c. PROGRAM ELEMENT NUMBER
62601F

6. AUTHORS
Gregory P. Ginet

5d. PROJECT NUMBER
1010

5e. TASK NUMBER
RR

5f. WORK UNIT NUMBER
A1

7. PERFORMING ORGANIZATION NAME(S) AND ADDRESS(ES)

Air Force Research Laboratory /VSBX
29 Randolph Road
Hanscom AFB, MA 01731-3010

8. PERFORMING ORGANIZATION REPORT NUMBER
AFRL-VS-HA-TR-2005-1178

9. SPONSORING/MONITORING AGENCY NAME(S) AND ADDRESS(ES)

10. SPONSOR/MONITOR'S ACRONYM(S)
AFRL/VSBX

11. SPONSOR/MONITOR'S REPORT NUMBER(S)

12. DISTRIBUTION/AVAILABILITY STATEMENT
Approved for public release; distribution unlimited.

13. SUPPLEMENTARY NOTES

14. ABSTRACT
Particle distributions measured near the magnetic equator are often mapped to higher latitudes to obtain estimates of global distributions. There are at least four sources of error in this mapping process: 1) neglect of the electric field term in the equation of motion, 2) the adiabatic invariant approximation to the equation of motion solution, 3) the inaccuracies of magnetic field models used to map fro a near-equatorial position to a lower altitude position along a magnetic field line, and the uncertainties generated by mapping measurements from an imperfect instrument. In the heart of the inner proton belt, the error is less than 10% for energies up to 10 MeV, 15% for 100 MeV, and 50% for 1 GeV. The error for electrons is less than 10% for energies from 10 keV to 100 MeV for radial positions less than 2.5 Re, and less than ~6% at the heart of the inner belt. These results indicate that in-situ flux measurements made by a near-equatorial satellite with arbitrarily high accuracy in energy and pitch angle could be used to create particle distribution functions at higher latitudes using standard mapping techniques with an error of order 105. The major limitation on both energy and angle measurement accuracy will be the contamination due to electrons and protons penetrating shielding, spreading in energy, and arriving at the detector at angles other than the nominal look angle.

15. SUBJECT TERMS
Radiation belts

16. SECURITY CLASSIFICATION OF: a. REPORT	b. ABSTRACT	c. THIS PAGE	17. LIMITATION OF ABSTRACT	18. NUMBER OF PAGES	19a. NAME OF RESPONSIBLE PERSON / 19B. TELEPHONE NUMBER *(Include area code)*
UNCL	UNCL	UNCL	SAR		Gregory P. Ginet / (781) 377-3974

Contents

Illustrations

Mapping Near-Equatorial Particle Distributions to Higher Latitudes: Estimates of Accuracy and Sensitivity

1. INTRODUCTION

The technique of mapping particle distributions measured near the magnetic equator to higher latitudes is often used to obtain estimates of the global distributions (e.g. Brautigam, et al. 1992; Gussenhoven, et al., 1993). In addition to the errors resulting from imperfect measurement of the near-equatorial distributions (e.g. finite energy range and angle of arrival determination) , inaccuracies are introduced into the global distributions through the mapping process. In this report an estimate is made of the mapping error as a function of location and particle energy. A general treatment estimating a "typical" error will be followed, rather than a comprehensive error budget analysis for a specific mission, instrument, and mapping procedure.

2. PARTICLE MAPPING

Particle mapping is performed in a magnetic coordinate space defined by $(L, s; \alpha, K)$ where L is the magnetic L-shell, defined as the distance from the center of the Earth to a magnetic field line along the magnetic equator; s is the distance along a magnetic field line from the magnetic equator; α is the pitch angle, defined as the angle between the particle's velocity components parallel and perpendicular to the magnetic field, and K is the particle kinetic energy (Figure 1). Measurements of the particle flux j at a point near the magnetic equator are mapped to a point further down the magnetic field at the same L, assuming there are no losses (K = constant), i.e.,

$$j(L,s_0;\alpha_0,K) \rightarrow j(L,s;\alpha,K) \tag{1}$$

where the fluxes at field line point s_0 and angle α_0 will map into fluxes at angle α at point s. The mapping is done according to solutions of the particle equation of motion,

$$\frac{d\mathbf{p}}{dt} = q\left(\mathbf{E} + \left(\frac{\mathbf{v}}{c} \times \mathbf{B}\right)\right) \tag{2}$$

where $\mathbf{p}$ is the momentum, $\mathbf{v}$ the velocity, q the charge, $\mathbf{E}$ the electric field, and $\mathbf{B}$ the magnetic field. For trapped radiation belt particles it is assumed that the magnetospheric electric field is negligible and the magnetic field is a dipole-like topology represented well by models containing an component from currents inside the Earth, such as the International Geophysical Reference Field (IGRF) and a component from

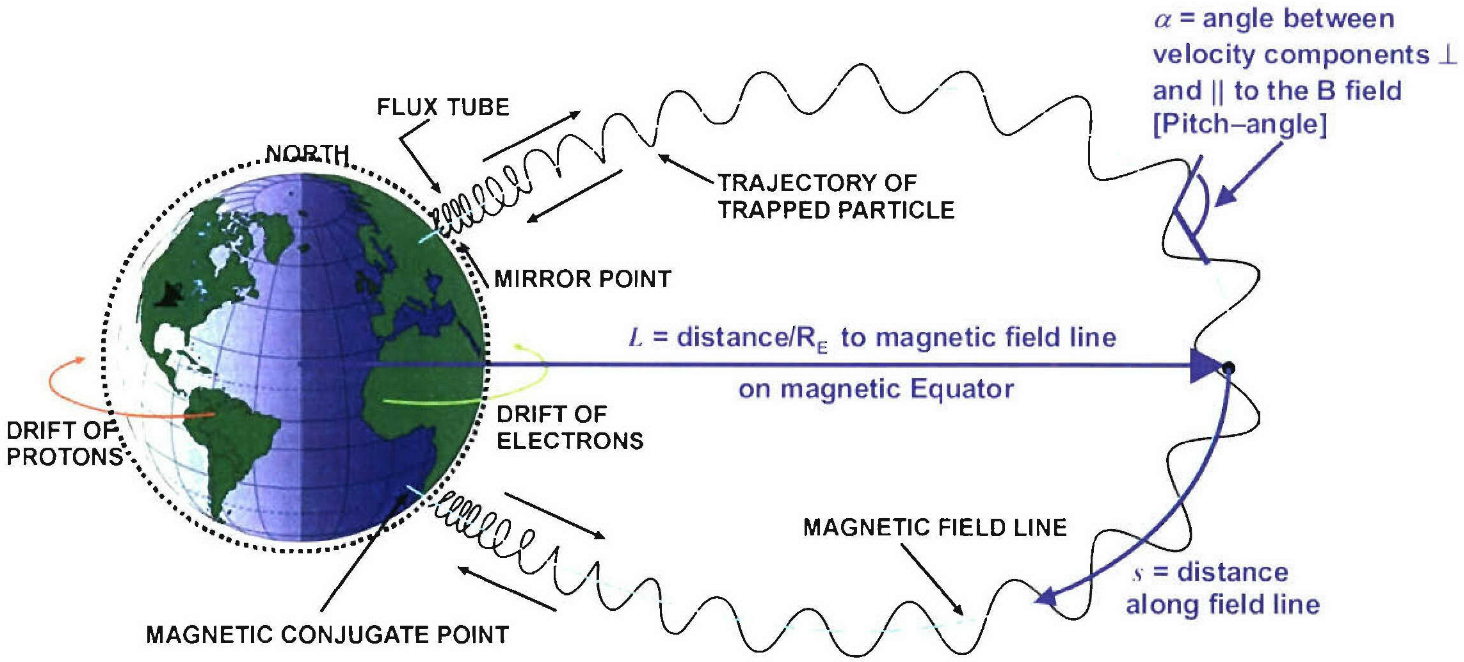

Figure 1. Magnetic Coordinate System Used for Particle Mapping in the Magnetosphere.

magnetospheric and ionospheric currents, such as Olson-Pfitzer 1977 or Tsyganenko 1989 (see Hilmer, 2001 for references). Furthermore, the solution to the equation of motion is assumed to preserve the adiabatic invariants corresponding to the standard cyclotron and bounce motions.

For example, in the case where the Earth's magnetic field is approximated by a dipole, the mapping is determined by the relation (cf. Lyons and Williams, 1984),

$$\frac{\sin^2\alpha}{B} = \frac{\sin^2\alpha_0}{B_0} \tag{3}$$

where B is the magnitude of the magnetic field at (L,s) and B_0 is the magnitude at the magnetic equator. The next section explores the degree to which each of the above assumptions is valid and the sensitivity to the magnetic field models chosen. Specific attention is given to the inner-magnetosphere, i.e. $1.0 < L < 3.0$, where the energetic inner proton belt lies.

3. ESTIMATES OF MAPPING ACCURACY

There are at least four sources of error in the mapping process described above: neglect of the electric field term in the equation of motion, the adiabatic invariant approximation to the equation of motion solution, the inaccuracies of magnetic field models used to map from a near-equatorial position to a lower altitude position along a field line, and the uncertainties generated by mapping measurements from an imperfect instrument. These sources are considered in turn below.

3.1. Magnetospheric Electric Fields

An estimate of the error, ε, involved in neglecting the electric field can be obtained by estimating the ratio of the electric to magnetic field terms on the right-hand-side of in the equation of motion [Eq. (2)],

$$\varepsilon_{Efield} = \left| \frac{\mathbf{E}}{\frac{\mathbf{v}}{c} \times \mathbf{B}} \right| \tag{4}$$

Defining $K = \gamma - 1$ to be the kinetic energy normalized to the rest mass, where γ is the usual relativistic factor, and assuming a dipole magnetic field where $|\mathbf{B}| \sim B_0 / L^3$ the above ratio can be written,

$$\varepsilon_{Efield} = 1.06 \times 10^{-5} \frac{(K+1)L^3}{[K(K+2)]^{1/2}} |\mathbf{E}| \text{ [mV/m]} \tag{5}$$

where $B_0 \sim 0.31$ gauss and the magnitude of the electric field is given in mV/m . A value of 1 mV/m will be used based on models of the average inner magnetospheric electric field derived from in-situ satellite data (Rowland and Wygant, 1998) which give this value as an upper bound except during rare large storms (when values up to 1.5 can be found).

Figure 2 shows the electric field error defined by Eq. (5) as a function of energy for several values of L for both protons (Figure 2a) and electrons (Figure 2b). In the inner magnetosphere the error is below 1% for protons above 1 MeV and well below 1% for electrons over the entire energy range considered.

3.2. Adiabatic Invariants

Invoking the adiabatic invariants as constants of the motion to approximate the solution of Eq. (2) requires that the cyclotron radius, ρ, of the particle be small compared to the scale length of the Earth's magnetic field, l_B. Assuming a dipole field, a typical scale length can be approximated as the inverse of the gradient of the radius of the field magnitude at the magnetic equator:

$$l_B \sim \frac{R_E}{3} \tag{6}$$

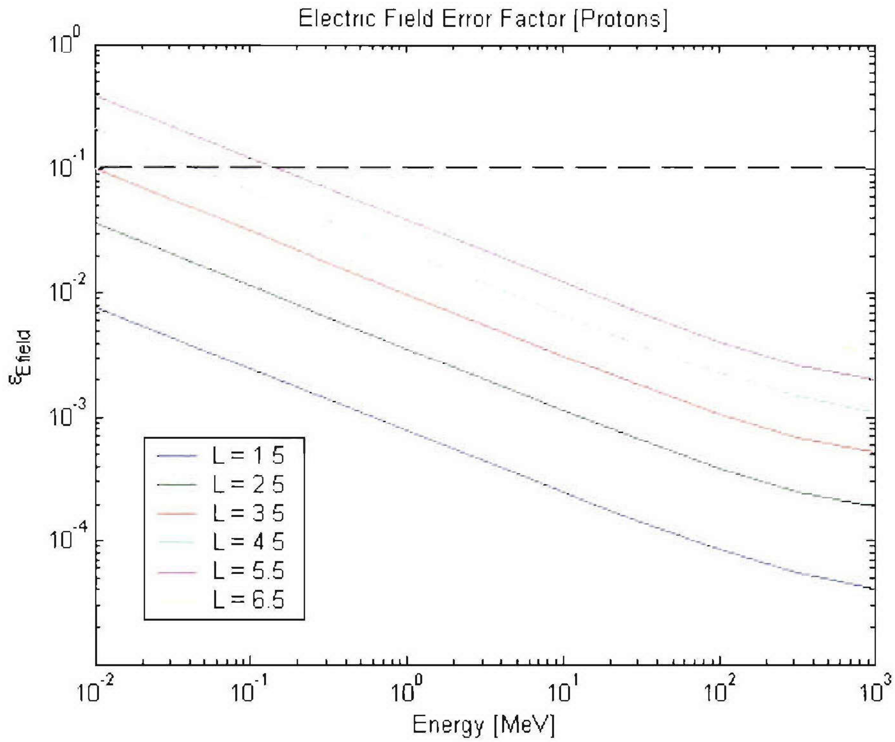

Figure 2a. Electric Field Error Factor for Protons as a Function of Energy from 10 keV to 1 GeV. Curves for several values of L from 1.5 to 6.5 are shown.

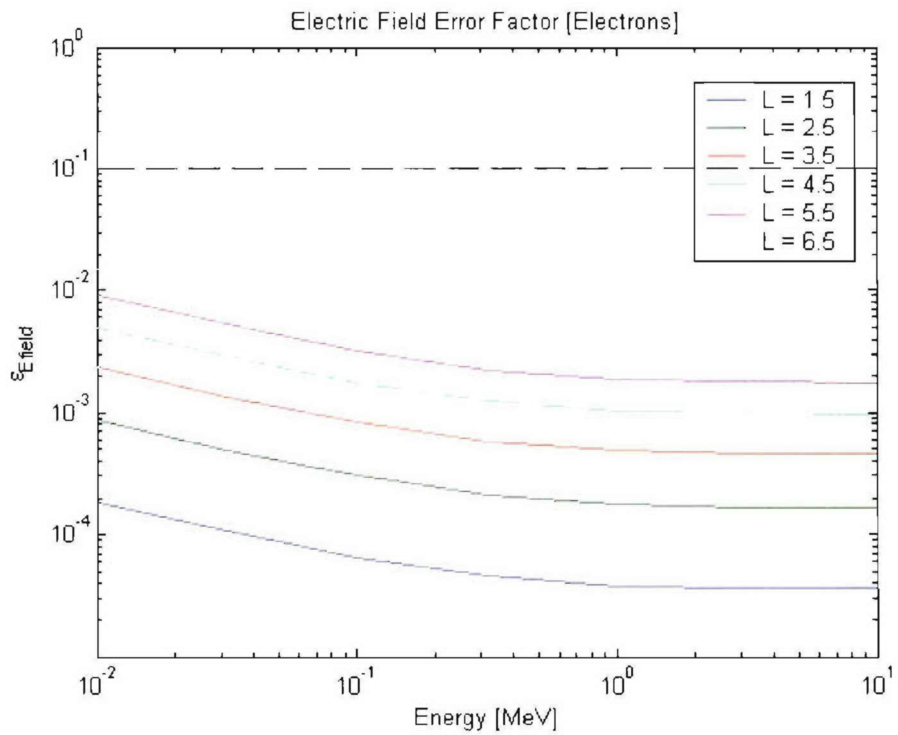

Figure 2b. Electric Field Error Factor for Electrons as a Function of Energy from 10 keV to 10 MeV (representative of the asymptotic values). Curves for several values of L from 1.5 to 6.5 are shown.

where R_E is the Earth's radius. With the cyclotron radius defined as:

$$\rho = \frac{v_\perp}{\Omega} = \frac{v_\perp}{c}\frac{\gamma mc^2}{q|\mathbf{B}|} \tag{7}$$

where m is the particle mass, $v_\perp$ is the velocity perpendicular to the magnetic field, and Ω is the cyclotron frequency, the adiabatic error can be estimated as:

$$\varepsilon_{Adiabatic} \sim \frac{3mc^2}{qB_0} L^2[K(K+2)]^{1/2} \tag{8}$$

where it is assumed that the entire particle velocity is perpendicular (an upper bound to ρ).

In Figure 3 the adiabatic invariant error is plotted as a function of energy for several values of L for both protons (Figure 3a) and electrons (Figure 3b). Errors for the electrons are less than 2% in the inner magnetosphere up to energies of 30 MeV, a value believed to be well beyond the energies characterizing the bulk of the distribution function. Protons, on the other hand, can have an error of up to 20% at $L \sim 3.0$ and energy of 100 MeV due to their relatively large cyclotron radius.

3.3 Magnetic Field Models

The sensitivity to using an imperfect magnetic field model can be estimated by comparing mapping results from two different magnetic field models in a typical region of interest. Figure 4 shows a cross section of the magnetosphere with field lines from both the IGRF '85/Olson-Pfitzer '77 (green) and IGRG '85/Tsyganenko '89 (purple) magnetic field models. Olson-Pfitzer represents an "average" magnetosphere while the Tysganenko model, driven with the magnetic index $K_p = 7$, represents a very active magnetosphere. Differences between the field configurations are reflective of variations due to geophysical activity as well as discrepancies in the modeling process itself since different methodologies were used in model construction. Shown also in Figure 4 are the inner and outer radiation belts as depicted by relative flux contours of the 36 MeV protons and 1.6 MeV electrons from the CRRESPRO Quiet and CRRESELE Average models, respectively (see Hilmer, 2001 for references).

Estimates of the mapping error will be made at a set of points P along a radial line at 0 degrees longitude and 30 degrees latitude as shown in Figure 4 (white line). The chosen latitude clips the horns of the inner belt protons but is sufficiently far off the magnetic equator to illustrate mapping inaccuracies. The following procedure is employed: (a) the magnetic field line from both of the models going through each of the points at 30 deg latitude is mapped to the geographic equator (red axis in Figure 4); (b) the radial separation between the two model predictions at the equator is used as an estimate for the difference in L at the magnetic equator, ΔL; (c) upper bounds to the gradient of

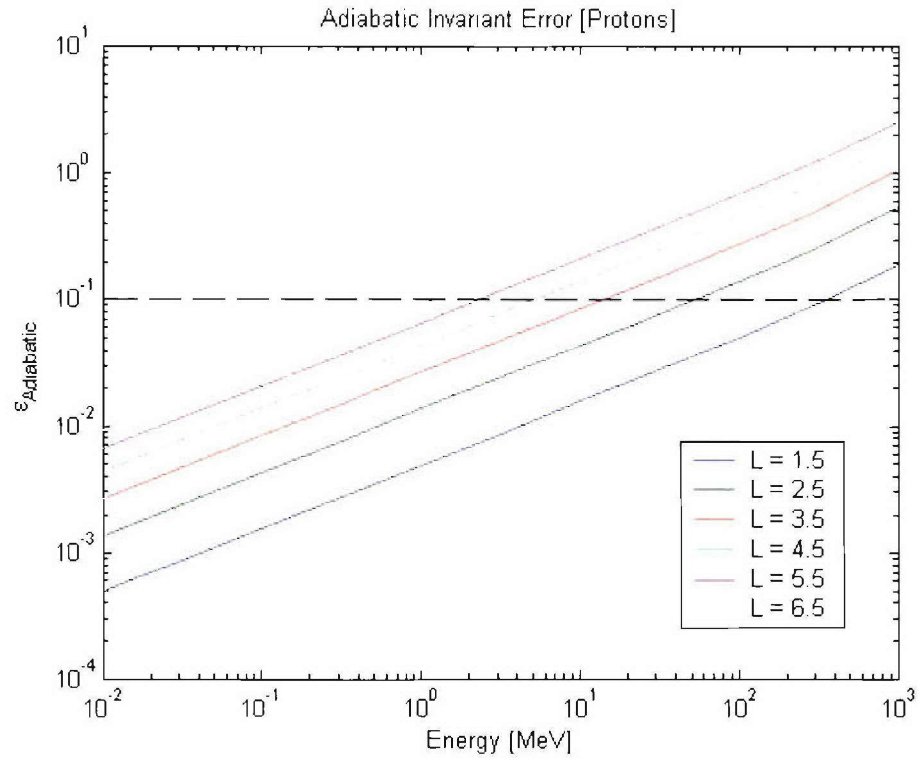

Figure 3a. Adiabatic Invariant Error Factor for Protons as a Function of Energy from 10 keV to 1 GeV. Curves for several values of L from 1.5 to 6.5 are shown.

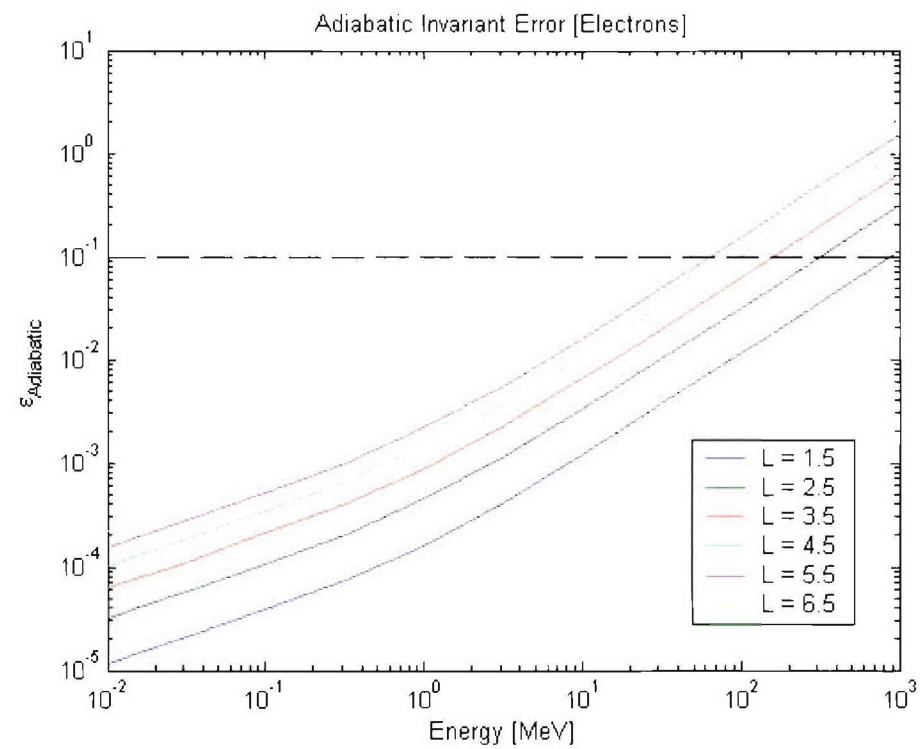

Figure 3b. Adiabatic Invariant Error Factor for Electrons as a Function of Energy from 10 keV to 1 GeV. Curves for several values of L from 1.5 to 6.5 are shown.

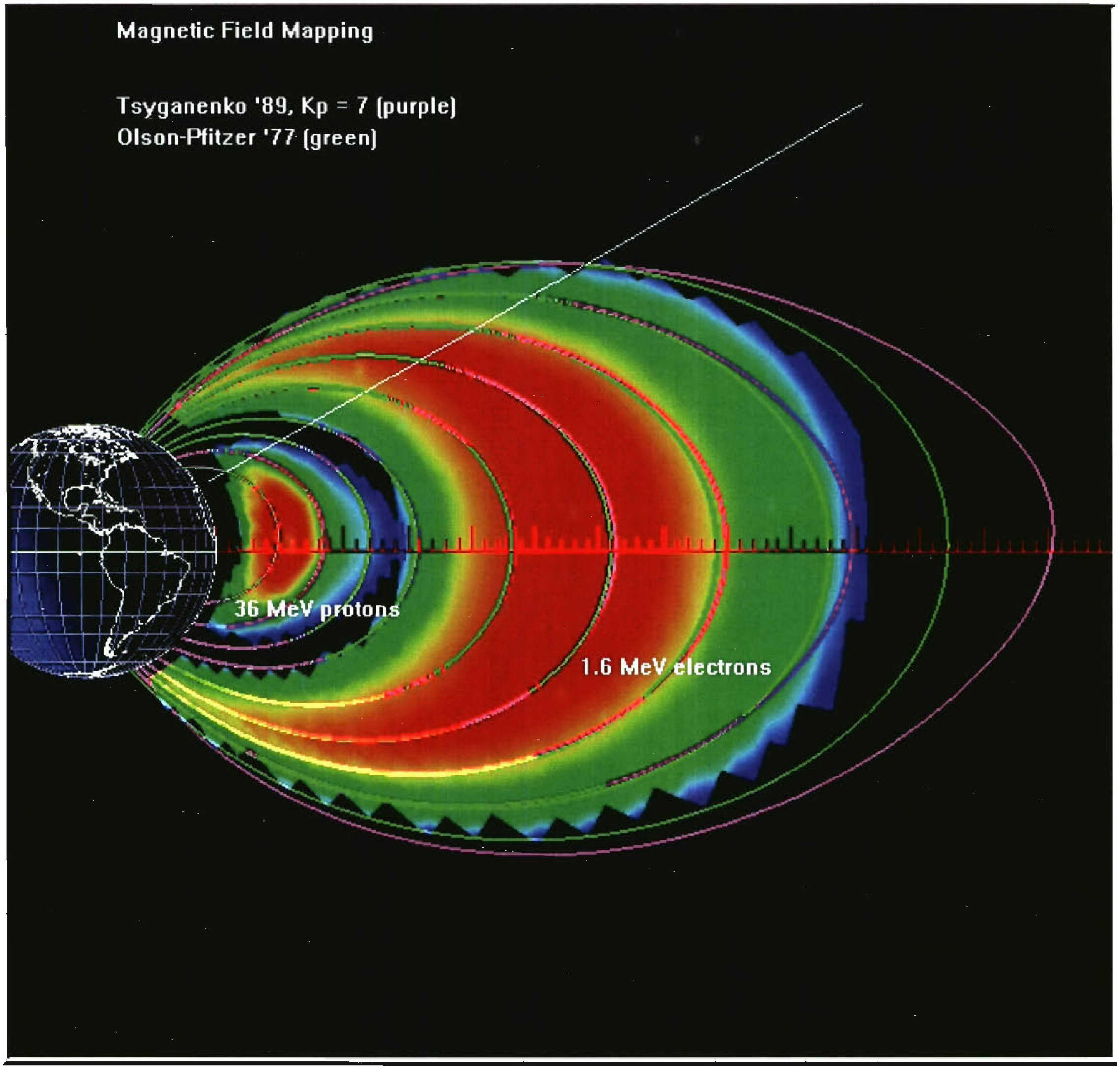

Figure 4. Cross Section of the Earth's Magnetosphere Showing Field Lines from the IGRF/Olson-Pfitzer '77 (green) and IGRF/Tysganenko '89 (purple) Models. Field lines from both models intersect along the 0 deg longitude, 30 deg latitude radial line (white.)

characteristic energetic proton and electron distributions along the equator are estimated; and finally (d) the relative error, ε_{Bfield}, of the particle flux along the 30 deg latitude line as determined by mapped measurements of the fluxes near the magnetic equator is estimated as,

$$\varepsilon_{Bfield} \sim \frac{\Delta L}{j(L_P)}\left|\frac{\partial j}{\partial L}\right|_{L_P} \tag{9}$$

where L_P is the L value corresponding to point P mapped to the magnetic equator using the IGRF/Olson-Pfitzer '77 model. Table 1 gives the points P, the mapped values L_P and the estimates of ΔL . Flux gradient estimates are obtained from radial differential energy flux profiles of the 36 MeV protons and 1.6 MeV electrons as given by the CRRESPRO quiet and CRRESELE average models, respectively (Figure 5). Fitting an exponential to the steepest part of the curves (shown by the red circles in Figure 5), that is, $j(L) \sim j_0 \exp\{aL\}$, where a is the inverse scale length, the relative error estimate can be written,

$$\varepsilon_{Bfield} \sim a\Delta L \tag{10}$$

where $a = 6.0$ (3.6) for the protons (electrons).

Figure 6 shows the mapping error estimate as a function of distance along a 30 deg latitude line for both the protons and electrons. Inner magnetosphere errors (P at radius = 2.5 Re corresponds to $L \sim 3.3$) are less than 10% for protons and electrons. This smallness is due to the domination of the relatively well modeled (by IGRF) internally generated magnetic field in the inner magnetosphere Note, however, that the error in IGRF itself has not been estimated and is assumed small compared to the error generated by the externally generated fields. Beyond $L \sim 3.5$ the error increases dramatically as a result of the less than perfectly understood and geophysically active nature of the external magnetic field.

Table 1. Values of P Along the 0 Degree Longitude, 30 Degree Latitude Line Used to Map the Model Magnetic Fields Together With Values for the Mapped L and Estimated ΔL Near the Magnetic Equator.

P (Re) at 0° long, 30° lat	L (IGRF/Olsen-Pfitzer map)	ΔL
1.25	1.4900	0.0020
1.50	1.8200	0.0045
1.75	2.2100	0.0100
2.00	2.5800	0.0125
2.50	3.3100	0.0150
3.00	4.1000	0.0400
3.50	4.9000	0.0800
4.00	5.8000	0.1800
4.50	6.7000	0.7900

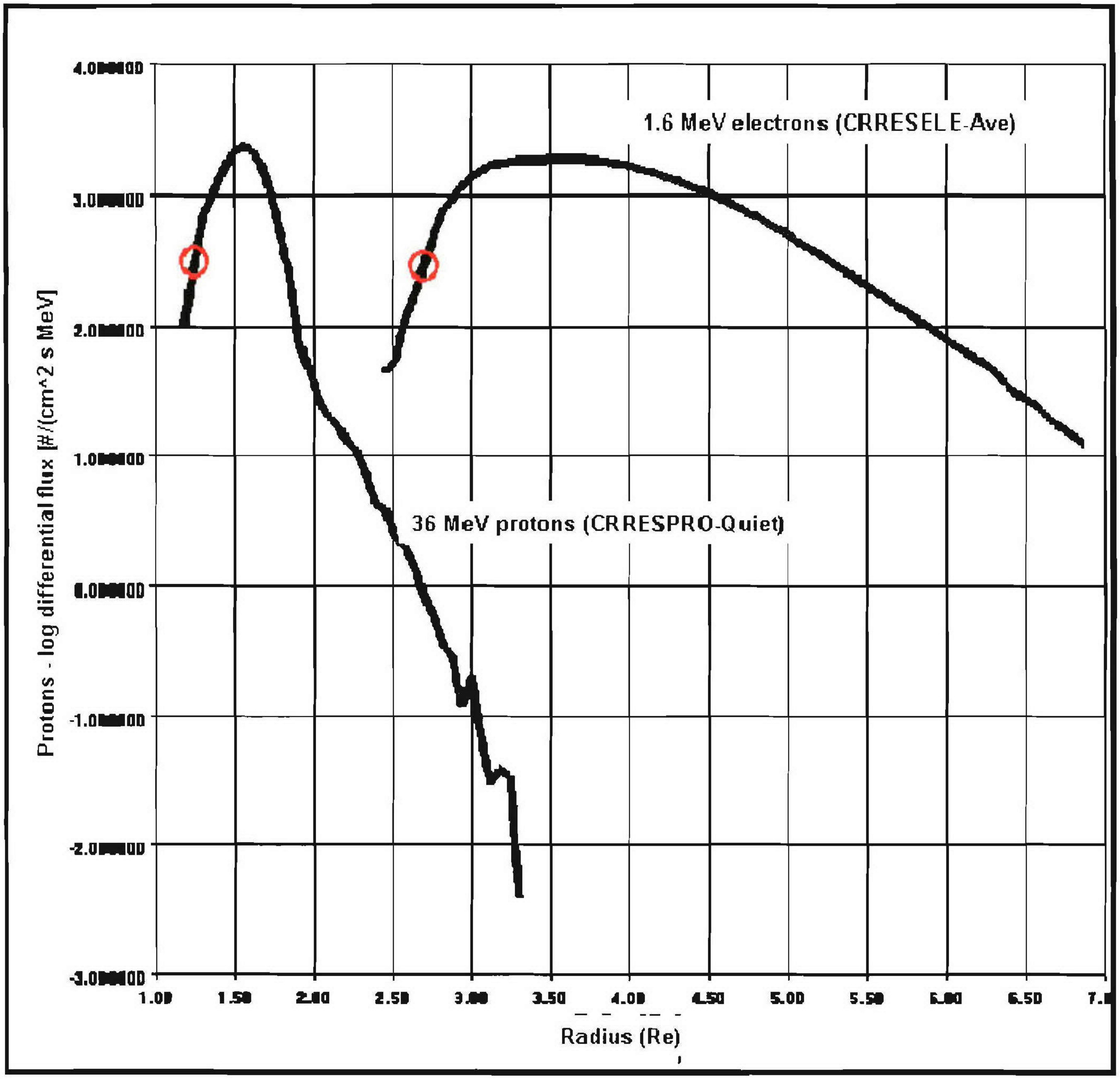

Figure 5. Radial Profiles Of the 36 Mev Protons and 1.6 Mev Electrons as Given by the CRRESPRO Quiet and CRRESELE Ave Models, Respectively. Red circles indicate the points used to estimate the maximum gradients.

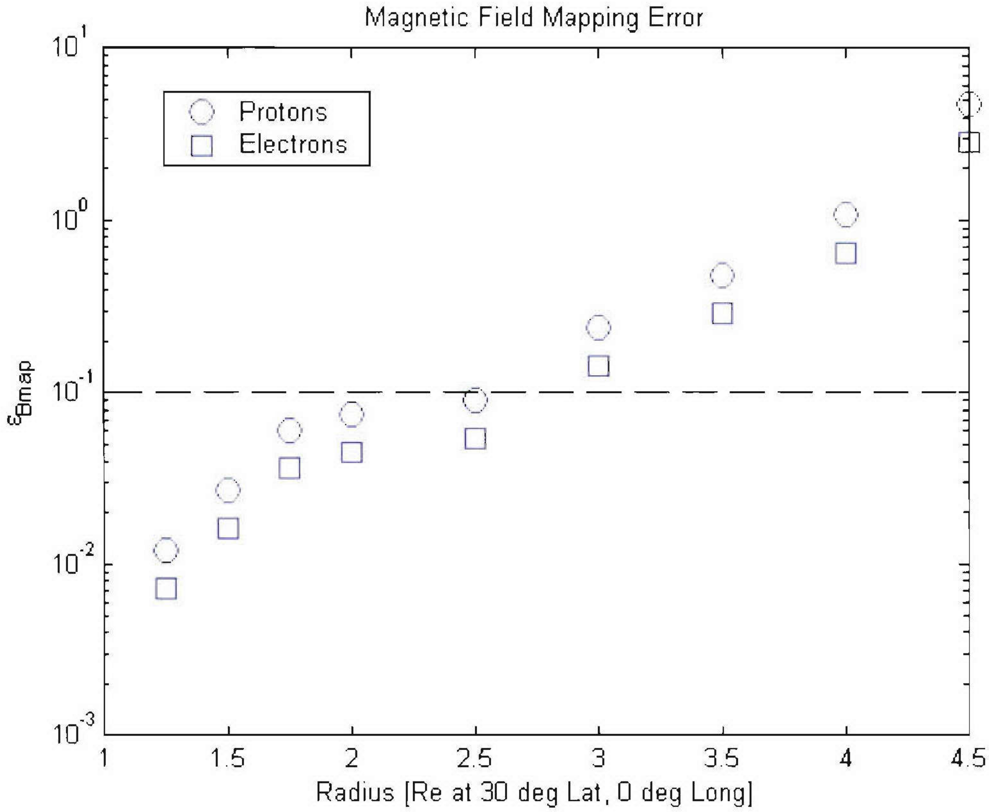

Figure 6. Error in Mapping due to Variations in Models as a Function of Radius Along the 0 Degree Longitude, 30 Degree Latitude Line.Magnetic Field

3.4. Mapping of Instrument Measurement Errors

Particle detectors do not provide arbitrarily precise and accurate measurements of equatorial energy and pitch angle. An uncertainty in energy range of 10% at the equator, for example, will map directly into a 10% energy range uncertainty off-equator due to the energy conserving nature of the mapping process. This is not true, however, of the pitch-angle mapping. Considering a dipole approximation to the Earth's magnetic field, the uncertainty $d\alpha$ at a point off the equator can be written in terms of the uncertainty $d\alpha_0$ at the equator by taking the differential of the mapping equation [Eq. (3)],

$$d\alpha = C_\alpha d\alpha_0 \tag{11}$$

where,

$$C_\alpha = \frac{\cos\alpha_0}{\left[\dfrac{\cos^6\lambda}{(1+3\sin^2\lambda)^{1/2}} - \sin^2\alpha_0\right]^{1/2}} \tag{12}$$

and λ is the magnetic latitude. There is a critical value of α_0 for each λ beyond which the denominator of Eq. (12) is imaginary and the mapping process is undefined. This is no surprise - this critical value corresponds to those particles that mirror at λ; particles with equatorial pitch angles above the critical value simply do not reach the specific off-equatorial point. In Figure 7 the pitch angle mapping factor C_α is plotted as a function of α_0 (in radians) for $\lambda = \pi/6$ (30 degrees). The critical value is $\alpha_0 \sim 0.6$ radian (~34 degrees) above which no particles make it to 30 degrees magnetic latitude. Below the critical values, the uncertainties $d\alpha_0$ will be amplified by the appropriate value of C_α. It is appropriate to view the amplification as a result of having to map only a portion of the equatorial pitch angle range (i.e. that below the critical angle) into the full $0 - \pi/2$ range accessible at the off equatorial point.

4. CONCLUSIONS

Neglecting the finite resolution of the instrument, the sum total of the error estimates $\varepsilon_{Efield} + \varepsilon_{Adiabatic} + \varepsilon_{Bfield}$ is plotted in Figure 8a (8b) for protons(electrons) as a function of radial position along the 0 degree longitude, 30 degree latitude line. Translations from the L-based estimates [Eqs. (5) and (8)] to the points P along the line are made using the field line mapping values in Table 1. For both protons and electrons, the error is monotonic in radius. Defining the outer boundary of the inner magnetosphere at a radius = 2.5 Re, corresponding to $L \sim 3.3$, results in an error for protons that is between 10 and 20% for energies up to ~ 10 MeV and then increases to ~ 33% at 100 MeV and ~ 100% at 1 GeV. In the heart of the inner proton belt at $L \sim 1.5 - 1.8$ (corresponding to radius = 1.25 - 1.5) the error is less than 10% for energies up to 10 MeV, reaches 15% for 100 MeV and is ~ 50% for 1 GeV. For electrons, the error is less than ~ 10% over 10keV- 100 MeV for radial positions less than 2.5 Re. At the heart of the inner belt the errors are less than ~ 6%.

In the context of a mission to map the inner magnetosphere, in particular protons and electrons in the inner belt with energies 1.0- 400 MeV and 0.5 - 30 MeV, respectively, the above results indicate that in-situ flux measurements made by a near-equatorial satellite with arbitrarily high accuracy in energy and pitch angle could be used to create particle distribution functions at higher latitudes using standard mapping techniques with an error of order 10%. With regards to the instrument uncertainties there will be an amplification of pitch angle measurement error as dictated by Eq. (11). The major limitation on both energy and angle measurement accuracy will not be the precision of the resolution but rather the contamination due to both electrons and protons penetrating shielding, spreading in energy, and arriving at the detector at angles other than the nominal look angle.

The relatively small mapping error for non-instrumental effects seems a price well worth paying for the additional spatial coverage provided by near-equatorial orbits compared to higher inclination orbits more characteristic of a particular operational environment. Constructing a contamination free instrument to provide sufficient energy and angle determination at the higher energies for both the in-situ fluxes and consequent mapped distributions will be the challenge.

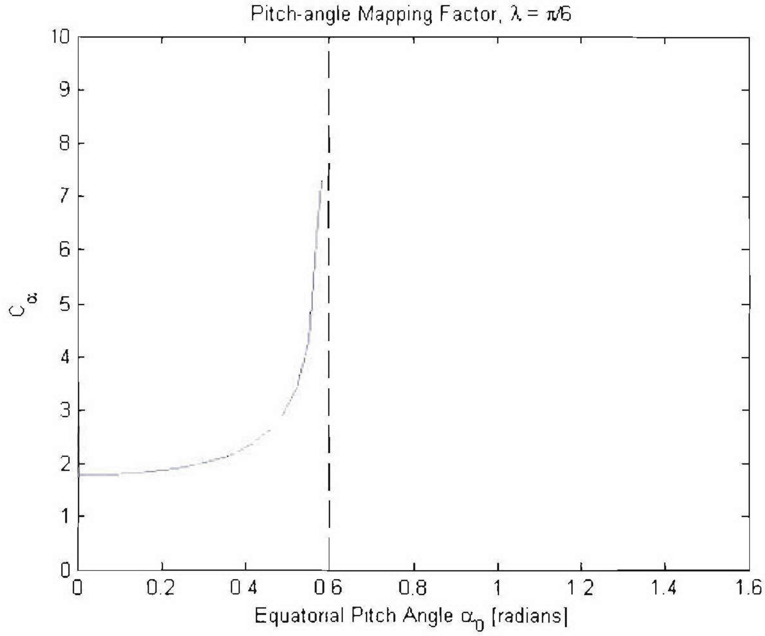

Figure 7. Pitch Angle Mapping Factor C_α as a Function of Equatorial Pitch Angle for Magnetic Co-Latitude of $\pi/6$ (30 degrees). The mirror angle is ~ 0.6 radians (~34 degrees).

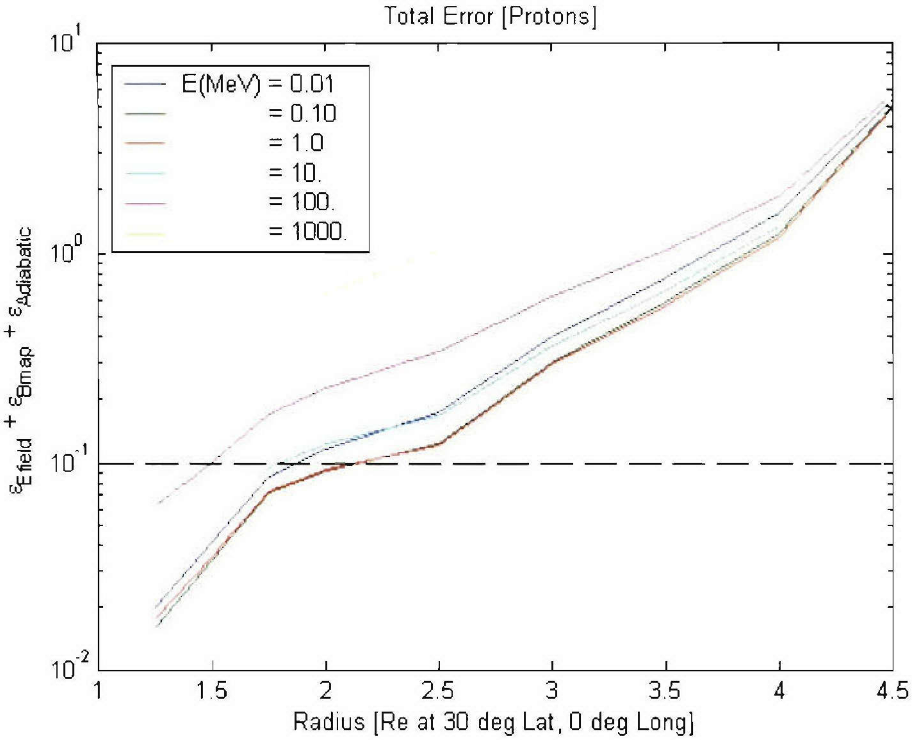

Figure 8a. Estimate of total mapping error for protons as a function of radius along the 0 degree longitude, 30 degree latitude line. Several curves in the energy range 10 keV to 1 GeV are given.

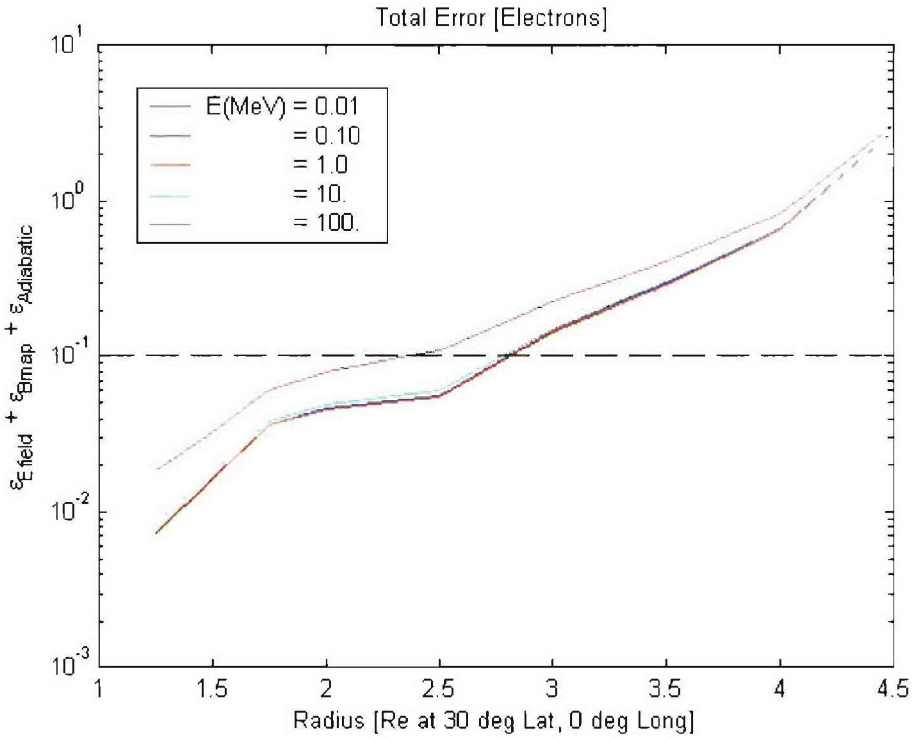

Figure 8b. Estimate of total mapping error for electrons as function of radius along the 0 degree longitude, 30 degree latitude line. Several curves in the energy range 10 keV to 100 MeV are given.

References

Brautigam, D.H., M.S. Gussenhoven, and E.G. Mullen, Quasi-static Model of the Outer Zone Electrons, *IEEE Trans. Nucl. Sci.,* **39**, 1797-1803, 1992.

Gussenhoven, M.S., E.G. Mullen, M.D. Violet, C. Hein, J. Bass, and D. Madden, CRRES High Energy Proton Flux Maps, *IEEE Trans. Nucl. Sci.*, **40**, 1450-1457, 1993.

Hilmer, R., Ed., *AF-GEOSpace User's Manual Version 2.0 and 2.0P*, update to AFRL-VS-TR-1999-1551 Special Reports, No. 281, available from AFRL (robert.hilmer@hanscom.af.mil), 2001.

Lyons, L. R. and D. J. Williams, *Quantitative Aspects of Magnetospheric Physics*, Reidel, Dordrecht, 1984.

Rowland, D. E. and J. R. Wygant, Dependence of the large-scale, inner magnetosphere electric field on geomagnetic activity, *J. Geophys. Res,* **108**, 14,959-14,964, 1998.